The Synthesis and Structure of Two Filled Skutterudite Compounds: $BaFe_4Sb_{12}$ and $BaRu_4Sb_{12}$

NED T. STETSON, SUSAN M. KAUZLARICH,* AND HÅKON HOPE

Department of Chemistry, University of California, Davis, California 95616

Two compounds, BaT_4Sb_{12} (T = Fe, Ru), have been synthesized using high temperature methods. These compounds crystallize in the cubic $LaFe_4P_{12}$ structure type. Two methods are described for the synthesis of $BaFe_4Sb_{12}$. Single crystals of $BaFe_4Sb_{12}$ can be prepared by reacting BaSb, Fe, and Sb in a 1:4:18 (Ba:Fe:Sb) molar ratio (method I). Single crystal X-ray diffraction data (room temperature, $a = 9.200(3)$ Å) for $BaFe_4Sb_{12}$ prepared by Method I were refined (cubic, $Im\bar{3}$ (No. 204), $Z = 2$, $R = 1.96\%$, $R_w = 1.73\%$ for 179 independent reflections). $BaFe_4Sb_{12}$ can also be prepared in $\geq 80\%$ yield from the reaction of stoichiometric amounts of Ba_2Sb_3, $FeSb_2$, and Sb (method II). Low temperature (130 K, $a = 9.188(2)$) single crystal X-ray diffraction data on $BaFe_4Sb_{12}$ crystals produced from Method II were also measured and refined ($R = 2.29\%$, $R_w = 2.45\%$ for 179 independent reflections). The structure of $BaFe_4Sb_{12}$ will be compared to that of the $LaFe_4Sb_{12}$ and $CoSb_3$. © 1991 Academic Press, Inc.

Introduction

Compounds of the composition LnT_4Pn_{12} (Ln = rare earth, Th; T = Fe, Ru, Os; Pn = P, As, Sb) have been known for a number of years (1–6). The $TPn_{6/2}$ framework is isostructural with the skutterudite ($CoAs_3$) structure. In these compounds there is a large interstitial site formed by the $TPn_{6/2}$ framework which is filled by a cation, hence the name filled skutterudite. In order for the filled skutterudite compounds, LnT_4Pn_{12}, to be isoelectronic with $CoAs_3$, a 4+ cation such as thorium is required (2). The majority of the compounds reported with the filled skutterudite structure contain a 3+ cation and are therefore somewhat electron deficient. In the case of Ln = Eu,

europium has been shown to be a 2+ cation (7, 8). More recently, the synthesis of three new compounds ($SrFe_4Sb_{12}$, $SrOs_4Sb_{12}$, and $BaRu_4Sb_{12}$) where the interstitial cation is a 2+ alkaline earth cation was reported (9). Most of the LnT_4Pn_{12} compounds are metallic (1–6), with the LaT_4P_{12} compounds being superconductors with transition temperatures of 4.1, 7.2, and 1.8 K for T = Fe, Ru, Os, respectively (10–12). No properties have been reported for the alkaline earth ternary compounds. In order to further investigate the chemistry of compounds of this structure type, we have synthesized the alkaline earth compound $BaRu_4Sb_{12}$, and the new compound $BaFe_4Sb_{12}$. In this paper we report the syntheses of these compounds and compare the structure and bonding of $BaFe_4Sb_{12}$ to the filled and empty skutterudite structures of $LaFe_4Sb_{12}$ and $CoSb_3$.

* To whom correspondence should be addressed.

Experimental

All reagents were stored and handled in a Vacuum Atmospheres dry box under a nitrogen atmosphere. Typical water levels were less than 0.2 ppm. Barium (99.9%), sublimed under argon, was obtained from Anderson Physics Laboratory. Iron powder (99.999%) and antimony shot (99.9999%) were obtained from Johnson Matthey. The ruthenium powder (Fisher) had no stated purity. The products were air stable and handled without further precaution.

$BaFe_4Sb_{12}$

Method I. The $BaFe_4Sb_{12}$ was initially synthesized using a modified version of the reported procedure for $LaFe_4Sb_{12}$ (6). A "BaSb" melt was prepared by arc melting a 1 : 1 molar mixture of the elements in an argon atmosphere. The black solid was easily ground and used in the synthesis of the ternary compounds. The BaSb, Fe, and Sb in a 1 : 4 : 18 (Ba : Fe : Sb) molar ratio were sealed in an evacuated quartz ampule. The mixture was heated to 900°C for 2 weeks and then quenched. The material was washed with acid. The X-ray powder diffraction pattern was analyzed and $BaFe_4Sb_{12}$ was identified, along with Sb, $FeSb_2$, and other minor impurities. From the powder diffraction data, $BaFe_4Sb_{12}$ was determined to be isostructural with $LaFe_4Sb_{12}$. Small, single crystals were isolated for a structure determination.

Method II. Subsequently, $BaFe_4Sb_{12}$ was prepared in $\geq 80\%$ yield (based on Guinier X-ray powder diffraction) from the binaries. The binary compounds, Ba_2Sb_3 (*13*) and $FeSb_2$ were synthesized by reacting the elements in an alumina crucible in a quartz ampule under 380 Torr of argon for 1–2 weeks. Reaction temperatures of 630 and 700°C were used for Ba_2Sb_3 and $FeSb_2$, respectively. Both of these binaries can be prepared quantitatively, indicated by Guinier X-ray powder diffraction. Ba_2Sb_3,

$FeSb_2$, and Sb were ground together into a fine powder in a 1 : 4 : 12 (Ba : Fe : Sb) molar ratio and pressed into a pellet. The pellet was sealed in an evacuated quartz ampule and reacted at 630–750°C for 1 week. The lower temperatures gave a powdered product while the higher temperatures produced crystals. The powder diffraction pattern shows a high yield of $BaFe_4Sb_{12}$ along with traces of Sb and $FeSb_2$. No Ba binary or ternary compounds other than BaT_4Sb_{12} have been identified.

$BaRu_4Sb_{12}$

The compound $BaRu_4Sb_{12}$ can be prepared in good yield using method I. Small amounts of Sb and $RuSb_2$ have been identified as minor impurities. No crystals have been grown for $BaRu_4Sb_{12}$.

Elemental Analysis

Elemental analysis was performed on several samples of BaT_4Sb_{12} using a Cameca SX50 microprobe. Assuming 4.00 atoms of T per formula unit, the results for the crystals prepared by method I were consistent with the stoichiometry $Ba_{0.84(6)}Fe_{4.00(8)}Sb_{11.8(2)}$. Analysis of several polycrystalline samples yielded $Ba_{0.95(3)}Fe_{4.00(6)}Sb_{11.7(1)}$. The analysis of crystals synthesized by method II were consistent with the stoichiometry $Ba_{0.95(4)}Fe_{4.00(3)}Sb_{11.9(2)}$. Microprobe data for polycrystalline samples of $BaRu_4Sb_{12}$ were consistent with the stoichiometry $Ba_{0.96(7)}Ru_{4.00(2)}Sb_{11.3(5)}$.

X-Ray Powder Diffraction

X-ray powder diffraction data were obtained using an Enraf-Nonius Guinier powder camera equipped with a quartz monochromator that gave clean $CuK\alpha_1$ radiation. Powdered silicon (NBS) was included in the samples as an internal standard, and the positions of the five observed lines were fit to known diffraction angles by a quadratic function. The lattice constants were then calculated by least-squares fit to indexed 2θ

values. The experimental diffraction positions and intensities agreed very well with the calculated diffraction pattern based on the single crystal X-ray structure for both $BaFe_4Sb_{12}$ and $BaRu_4Sb_{12}$. The lattice parameters obtained at room temperature were 9.200(2) Å (method I) and 9.206(2) (method II) for the Fe compound and 9.312(1) Å for the Ru compound.

Single Crystal X-Ray Diffraction

Single crystal X-ray diffraction analysis of a silver, trigonal pyramid-shaped crystal (dimensions 0.125 × 0.125 × 0.075 mm) obtained from method I was initially carried out at 130 K on a Syntex $P2_1$ diffractometer. The structure was refined using SHELXTL Version 5.0 installed on a Data General Eclipse computer.

The unit cell is consistent with I-centered cubic with a = 9.184(2) Å. The systematic absences are consistent with six space groups, but $Im\overline{3}$ was chosen for the solution since it corresponds to the highest symmetry and is the accepted space group for the $LaFe_4Sb_{12}$ structure. Merging of the data in this space group gave an R_{merge} value of 0.127, much higher than expected. The other space groups either gave the same or higher R_{merge} values. Initial atom positions were obtained from direct methods. After two absorption corrections (14, 15) and refinement of the structure with isotropic Us for the Fe and Ba atoms and anisotropic Us for the Sb atom, the R was 7.39% (R_w = 7.75%). The largest peak in the difference map was 6.6 e/Å^3. This was an unacceptable refinement result. Inspection of the raw data file revealed relatively large discrepancies in intensity for equivalent reflections.

To determine if the discrepancies in intensity for equivalent reflections were due to absorption or twinning (16, 17), X-ray data were collected on a Siemens R3/V diffractometer (Mo$K\alpha$ radiation, λ = 0.71073 Å, room temperature) from a second, needle-shaped crystal with a silver reflection (dimensions 0.05 × 0.05 × 0.15 mm). The full

TABLE I

DATA COLLECTION AND REFINEMENT PARAMETERS FOR $BaFe_4Sb_{12}$

T	298 K	130 K
Z	2	2
Space group	$Im\overline{3}$	$Im\overline{3}$
a (Å)	9.200(3)	9.188(2)
V (Å^3)	780.4(7)	775.6(7)
d_{calc} (Mg · m^{-3})	7.653 (Ba occ. 83%)^a	7.770 (Ba occ. 92%)^a
Monochromator	Highly oriented graphite	Zr filter
μ (Mo $K\alpha$), mm^{-1}	26.17	26.78
Range of transmission factors	9–34%	6–13%
Scan method	ω, 1.2° range, 1° offset for bkgd	2θ–θ, (α_1–0.7) to (α_2 + 0.7)
Scan speed	20°/min in ω	60°/min in 2θ
Weighting scheme	$w^{-1} = \sigma^2(F)$	$w^{-1} = \sigma^2(F)$
Refinement method	Full-matrix least squares	Full-matrix least squares
Quantity minimized	$\Sigma w(F_0 - F_c)^2$	$\Sigma w(F_0 - F_c)^2$
No. of parameters refined	12	12
R	0.0196	0.0229
R_w	0.0173	0.0245

^{a} d_{calc} (Mg · m^{-3}) = 7.755 (Ba occ. 100%).

diffraction sphere was collected to 2θ = 55° (3563 reflections). The data collection and refinement parameters are given in Table I. The data set was processed with SHELTXL PLUS (Release 3.43) on a MicroVAX computer. An empirical absorption correction (18), making use of I_0 for equivalent reflections to determine an absorption correction function, was applied to the complete data set (3563 reflections). The data set was merged (R_{merge} = 6.42%, 179 independent reflections) and the initial positions of Ba, Fe, and Sb were taken from the first data set. All atoms were refined with anisotropic Us, and the Ba occupancy was allowed to refine to give a final R of 1.96% (R_w = 1.73%). The final difference map was flat to ±1.5 e/Å^3. The discrepancies in intensities in the raw data set are attributed to absorption, and not to twinning (16, 17). Table II provides positional and thermal parameters. Listing of the observed and calculated structure factor amplitudes are available from an author (S.M.K.) on request.

Single crystal X-ray diffraction analysis of a rectangular-shaped crystal (dimensions

TABLE II

POSITIONAL PARAMETERS AND DISPLACEMENT COEFFICIENTS ($\mathring{A}^2 \times 10^4$) FOR BaFe₄Sb₁₂

		Ba		Sb		Fe	
	T:	298 K	130 K	298 K	130 K	298 K	130 K
x		0		0.16080(4)	0.16113(5)	0.25	
y		0		0.33955(4)	0.34011(5)	0.25	
z		0		0		0.25	
U(equiv)[a]		102(3)	68(3)	83(1)	66(2)	64(2)	66(5)
U_{11}[b]		102(5)	68(6)	81(2)	67(4)	64(3)	66(5)
U_{22}		102(5)	68(6)	105(3)	75(4)	64(3)	66(5)
U_{33}		102(5)	68(6)	62(2)	57(4)	64(3)	66(5)
U_{23}		0		0		2(3)	5(3)
U_{13}		0		0		2(3)	5(3)
U_{12}		0		7(1)	2(1)	2(3)	5(3)
Occupancy		0.0351(3)	0.0384(4)	0.5		0.16667	
		(84%)	(92%)	(100%)		(100%)	

[a] Equivalent isotropic U defined as one-third of the trace of the orthogonalized U_{ij} tensor.

[b] The anisotropic temperature factor exponent takes the form: $-2\pi^2(h^2a^{*2}U_{11} + ... + 2hka^*b^*U_{12})$.

0.04 × 0.1 × 0.16 mm) obtained from method II were measured at 130 K on a Siemens R3mRA with a rotating anode source (Zr-filtered Mo$K\alpha$ radiation, $\lambda = 0.71073$ Å, 15 kW). Three ψ scans at different 2θ values showed approximately 53% variation in intensity. A total of 3566 reflections were collected for a full diffraction sphere to $2\theta = 55°$. The data collection and refinement parameters are given in Table I. The structure was refined as described above (179 reflections, $R_{merge} = 3.89\%$) to give a final R of 2.29% ($R_w = 2.45\%$). The final difference map was flat to ±2.3 e/A³. The occupancy for the Ba atom refined to 92.0(7)%. Table II provides positional and thermal parameters. Listing of the observed and calculated structure factor amplitudes are available from an author (S.M.K.) on request.

Results and Discussion

Method I gave low yields for BaFe₄Sb₁₂ and required the use of excess Sb. The single crystals obtained were too small for property measurements and the excess Sb and impurities could not be totally removed by acid washing. The product was resistant to concentrated HNO₃ or HCl, but was attacked by a mixture of the two. The purity level could be improved by acid washings, but the impurities were never totally removed. When the synthesis was attempted without excess Sb, no BaFe₄Sb₁₂ was produced. To avoid these problems, method II was developed; it gives much improved yields. This improvement is attributed to the more uniform mixing that is achieved by using the binaries as starting reagents. Method II requires lower temperatures than method I. The melting and/or decomposition temperatures for each of these binaries are within the temperature range of 630–750°C, thus increasing the reactivity of the starting reagents at lower temperatures. The microprobe data and single crystal X-ray diffraction data indicate that the crystals obtained from method II are higher in Ba content than the crystals obtained from method I.

The filled skutterudite structure has been described previously (5). Table III compares the bond distances and angles (both

TABLE III

IMPORTANT BOND DISTANCES (Å) AND ANGLES (°) FOR $CoSb_3$, $LaFe_4Sb_{12}$, AND $BaFe_4Sb_{12}$

	$CoSb_3$[a]	$LaFe_4Sb_{12}$[b]	$T:$	$BaFe_4Sb_{12}$ 298 K	130 K
Distances					
$M-Sb^c$	2.520	2.554(2)		2.577(1)	2.574(1)
Sb–Sb	2.891	2.932(2)		2.952(1)	2.937(1)
	2.982	2.980(2)		2.959(1)	2.960(1)
$A-Sb^d$		3.411(2)		3.456(1)	3.457(1)
Sb ⋯ 4Sb	3.415	3.443(2)		3.452(1)	3.442(1)
Angles					
Sb–M–Sb^c	85.3	84.8(1)		84.1(1)	83.9(1)
	94.7	95.2(1)		95.9(1)	96.1(1)
M–Sb–M^c	127.3	126.9(1)		126.4(1)	126.3(1)
M–Sb–Sb^c	107.7	108.1(1)		108.6(1)	108.5(1)
	108.8	108.7(1)		108.6(1)	108.8(1)

[a] Ref (19).
[b] Ref (4).
[c] M = Co, Fe.
[d] A = La, Ba.

FIG. 1. A view of the skutterudite structure showing the $FePn_{6/2}$ octahedra.

room temperature (298 K) and low temperature (130 K)) found in $BaFe_4Sb_{12}$ with $LaFe_4Sb_{12}$ (4) and $CoSb_3$ (19). The structure is best described as slightly distorted, corner-sharing $FeSb_{6/2}$ octahedra. Figure 1 shows the connectivity of the octahedra. The Fe–Sb bond (2.577 Å) is slightly longer than that observed for $LaFe_4Sb_{12}$ (2.554 Å) (4), but agrees well with the Fe–Sb bond lengths of 2.575 and 2.598 Å observed in $FeSb_2$ (20). The octahedra are tilted so that the Sb atoms form an Sb_4 ring in 3/4 of the body center sites formed by the cubic Fe atom lattice. The other 1/4 of the body center sites are occupied by the Ba cation. Each octahedron is connected to each adjacent octahedron by one side of the two of the Sb_4 rings in addition to the shared corner. These Sb_4 rings can be clearly seen in the extended ($FeSb_{6/2}$) framework shown in Fig. 2. The inner angles of the rings are 90°, and the rings are planar. The Sb–Sb bond distances, 2.952(1) Å and 2.959(1) Å, make these rings almost perfect squares in $BaFe_4Sb_{12}$. In $LaFe_4Sb_{12}$, the Sb–Sb distances are 2.932(2)

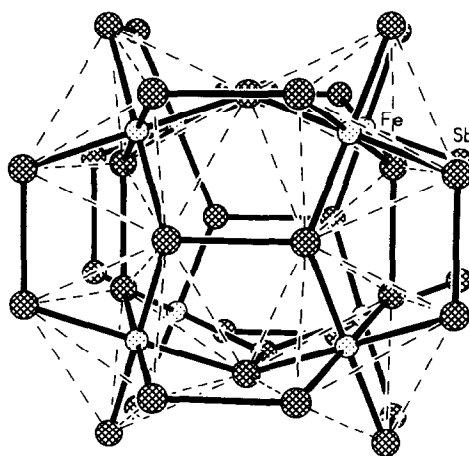Å and 2.980(2) Å, and in $CoSb_3$ the distances are 2.891 Å and 2.982 Å. The Sb–Sb bonds in these Sb_4 rings in both the skutterudite and the filled skutterudite structures are somewhat longer than typically observed in the transition metal binary compounds such
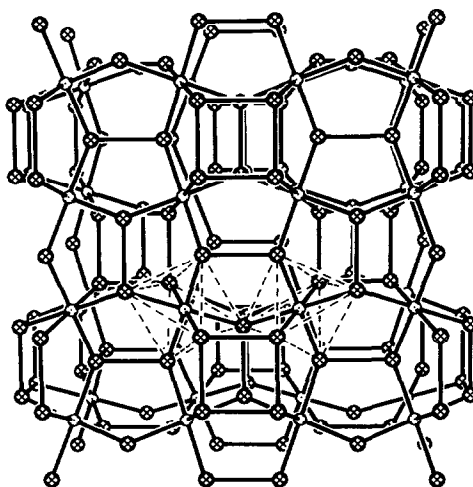

FIG. 2. A view of the extended Fe–Sb framework. The unit cell and two $FeSb_{6/2}$ octahedra is outlined.

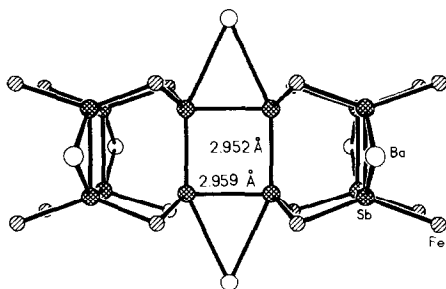FIG. 3. A view of the Sb$_4$ rings with important distances shown.

as MSb$_2$ (M = Cr, Fe, Ni, Ru, and Os) (21).
Typical Sb–Sb bond distances in FeSb$_2$ (20)
are 2.89 Å, compared to 2.89–2.98 Å in
CoSb$_3$ (19). Both LaFe$_4$Sb$_{12}$ and BaFe$_4$Sb$_{12}$
have somewhat longer Sb–Sb bond lengths
(2.93–2.98 Å), with the average Sb–Sb bond
length being about equal (2.956 Å). These
Sb$_4$ rings run orthogonal to each other along
each crystallographic axis. Figure 3 shows
an Sb$_4$ ring with two orthogonal Sb$_4$ rings,
both the Ba cations and the Fe atoms are
included. The interring Sb···4Sb distance of
3.452(1) Å is almost identical to the interring
Sb···4Sb distance of 3.443(2) Å observed in
LaFe$_4$Sb$_{12}$. It is interesting to note that these

rings become distorted at 130 K with Sb–Sb
distances of 2.937(1) Å and 2.960(1) Å. The
center of the cell shown in Figs. 1 and 2 is
empty as it would be for the skutterudite
structure. It is this interstitial site in the filled
skutterudite structure that contains an elec-
tropositive cation. The Ba coordinates to
one side of the rings in each of the six adja-
cent sites, giving it a coordination number
of 12 (Fig. 4). The Ba–Sb distances are
3.456(1) Å; this is about the same as the
Ba–Sb distances of 3.461–3.759 Å observed
in the binary compound Ba$_2$Sb$_3$ (13). The
thermal parameters for the Ba atoms are
somewhat larger than for the Sb atoms, but
the relative difference between these param-
eters is not nearly as large as it is for La and
Sb in LaFe$_4$Sb$_{12}$ (4). The interstitial site is
about 84–95% occupied in BaFe$_4$Sb$_{12}$ de-
pending upon the reaction procedure and
may be approximately 94% occupied in
LaFe$_4$Sb$_{12}$ (4). In BaFe$_4$Sb$_{12}$ the nonstoichi-
ometry of the Ba ions is confirmed by micro-
probe analysis of polished single crystals.
The X-ray results are consistent with the
higher Ba content for a crystal prepared by
method II as observed in the microprobe
analysis with the interstitial site being about
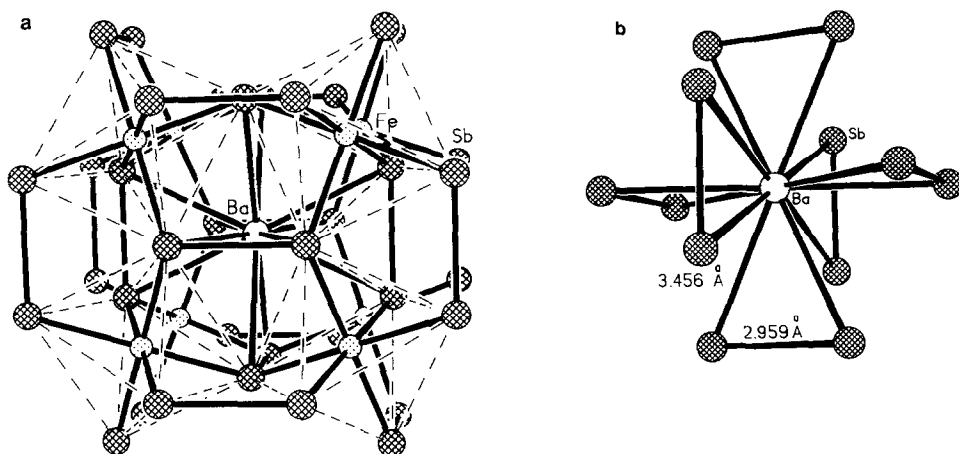92–95% occupied.

FIG. 4. (a) A view of the filled skutterudite structure. (b) The Ba–Sb coordination; important bond distances are shown.
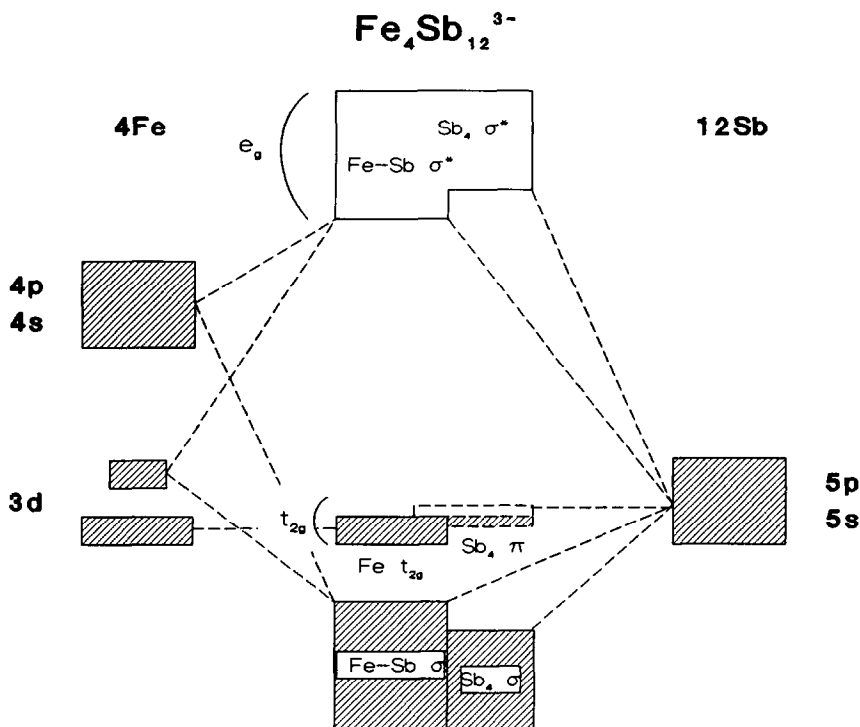
$$Fe_4Sb_{12}{}^{3-}$$

FIG. 5. A schematic MO energy-level diagram for the polyanion $Fe_4Sb_{12}^{3-}$ based on Ref. (23).

LaFe$_4$Sb$_{12}$ and BaFe$_4$Sb$_{12}$ can be described as La(FeSb$_{6/2}$)$_4$ and Ba(FeSb$_{6/2}$)$_4$, respectively. The FeSb$_{6/2}$ framework is isostructural to CoSb$_3$, but is electron deficient compared with CoSb$_3$. LaFe$_4$Sb$_{12}$ is reported to be metallic (1, 4). The metallic conductivity may be due to the nonstoichiometry associated with the La ion occupancy (4), but LaFe$_4$Sb$_{12}$ is expected to be metallic even if the interstitial site were completely filled, since the skutterudite framework, Fe$_4$Sb$_{12}^{3-}$, is one electron deficient. As the interstitial cation is changed from La to Ba, there is one less electron donated from the cation to the skutterudite framework giving Fe$_4$Sb$_{12}^{2-}$. A simple band structure for the skutterudite structure has been previously proposed (1–5, 22) and two theoretical calculations on the bonding of LaFe$_4$P$_{12}$ have been recently published (23, 24). Although the simple band structures that have been proposed appear to be essen-

tially correct (1, 5), the theoretical calculations provide more detail and a greater understanding of the structure and properties (23, 24). The extended Hückel calculations (23) show that near the top of the Fermi level lie the t_{2g} block orbitals of the transition metal, which are essentially nonbonding and filled. In the case of Pn = P, the highest occupied (HO) band is primarily Pn–Pn in character and overlaps with the t_{2g} metal orbitals. There is a large gap between the filled t_{2g} block band and the empty e_g block band. This is shown schematically in Fig. 5. In the case of CoSb$_3$, all the M–Sb, Sb$_4$ σ and the t_{2g} block bands are filled. This would be consistent with CoSb$_3$ being a diamagnetic semiconductor (25). For LaFe$_4$Sb$_{12}$, the M–Sb, Sb$_4$ σ bands are filled and the t_{2g} block band is one electron deficient. The extended Hückel calculations (23) show the top of the HO band to be primarily Pn–Pn π antibonding in character for Fe$_4$Pn$_{12}^{3-}$.

If the HO band is primarily *Pn–Pn* antibonding in character, then the removal of electrons would effect the *Pn–Pn* bonding as is observed: the Sb_4 rings are rectangular for $LaFe_4Sb_{12}$ and $CoSb_3$ and square for $BaFe_4Sb_{12}$. There is also a slight elongation of the *M*–Sb bond going from $CoSb_3$ with the *M*–Sb bond length of 2.52 to 2.55 Å for $LaFe_4Sb_{12}$ and 2.58 Å for $BaFe_4Sb_{12}$. This may be due to attractive interactions between the cation and the Sb anions.

The properties of $BaFe_4Sb_{12}$ and $BaRu_4Sb_{12}$ are currently under investigation and will provide further insight into the electronic structure of the filled skutterudite compounds. These compounds appear to be nonstoichiometric and this complicates the interpretation of both the structure and the properties within this series. The Sb_4 rings in $BaFe_4Sb_{12}$ are nearly square at room temperature and are rectangular at 130 K. In the case of $BaFe_4Sb_{12}$, the interstitial site is about 84–95% filled depending on the reaction procedure. Since the EuT_4P_{12} compounds can be prepared and the europium cation has been determined to be a 2 + cation (7, 8), it is expected that $A^{II}T_4P_{12}$, where A = alkaline earth cation, can also be prepared. Calculations on LaT_4P_{12} indicate that both the interstitial cation and the *Pn* framework are important in determining the superconducting properties (23, 24). Synthesis of the $A^{II}T_4P_{12}$ compounds are underway and may provide additional insight into the superconducting properties of the LaT_4P_{12} compounds.

References

1. F. GRANDJEAN, A. GÉRARD, D. J. BRAUN, AND W. JEITSCHKO, *J. Phys. Chem. Solids* **45**, 877 (1984).
2. D. J. BRAUN AND W. JEITSCHKO, *J. Less-Common Met.* **76**, 33 (1980).
3. D. J. BRAUN AND W. JEITSCHKO, *J. Solid State Chem.* **32**, 357 (1980).
4. D. J. BRAUN AND W. JEITSCHKO, *J. Less-Common Met.* **72**, 147 (1980).
5. W. JEITSCHKO AND D. BRAUN, *Acta Crystallogr. Sect. B* **33**, 3401 (1977).
6. G. P. MEISNER, M. S. TORKACHVILI, K. N. YANG, M. B. MAPLE, AND R. P. GUERTIN, *J. Appl. Phys.* **57**, 3073 (1985).
7. A. GÉRARD, F. GRANDJEAN, J. A. HODGES, D. J. BRAUN, AND W. JEITSCHKO, *J. Phys. C* **16**, 2797 (1983).
8. F. GRANDJEAN, A. GÉRARD, J. HODGES, D. J. BRAUN, AND W. JEITSCHKO, *Hyperfine Interact.* **15/16**, 765 (1983).
9. L. BOONK, W. JEITSCHKO, U. D. SCHOLZ, AND D. J. BRAUN, *Z. Kristallogr.* **178**, 30 (1987).
10. L. E. DELONG AND G. P. MEISNER, *Solid State Commun.* **53**, 119 (1985).
11. G. K. SHENOY, D. R. NOAKES, AND G. P. MEISNER, *J. Appl. Phys.* **53**, 2628 (1982).
12. G. P. MEISNER, *Physica* **108B**, 763 (1981).
13. B. EISENMANN, H. JORDAN, AND H. SCHÄFER, *Z. Naturforsch.* **40b**, 1603 (1985).
14. Neutral atom scattering factors and corrections for anomalous dispersion are from the "International Tables for X-ray Crystallography" Vol. IV, Kynoch Press, Birmingham, England (1974).
15. The absorption correction is made using Program XABS, H. Hope and B. Moezzi. The program obtains an absorption tensor from $F_0–F_c$ differences. B. Moezzi, PhD dissertation, University of California, Davis, 1987.
16. A. SANTORO, *Acta Crystallogr. Sect. A* **30**, 224 (1974).
17. Y. LE PAGE, J. D. H. DONNAY, AND G. DONNAY, *Acta Crystallogr. Sect. A* **40**, 679 (1984).
18. XEMP-Empirical absorption correction, SHELXTL PLUS-Release 4.11/V.
19. A. KJEKSHUS AND T. RAKKE, *Acta Chem. Scand.* **A28**, 99 (1974).
20. H. HOLSETH AND A. KJEKSHUS, *Acta Chem. Scand.* **23**, 3043 (1969).
21. H. HOLSETH AND A. KJEKSHUS, *Acta Chem. Scand.* **22**, 3284 (1968).
22. J. ACKERMANN AND A. WOLD, *J. Phys. Chem. Solids* **38**, 1013 (1977).
23. D. JUNG, M.-H. WHANGBO, AND S. ALVAREZ, *Inorg. Chem.* **29**, 2252 (1990).
24. R. B. KING, *Inorg. Chem.* **28**, 3048 (1989).
25. G. KLICHE AND W. BAUHOFER, *J. Phys. Chem. Solids* **49**, 267 (1988).